Superconductor photonic crystal: Optical tunable multichannel filter

V. R. BALAJI[1], VIGNESWARAN DHASARATHAN[2,*], SOFYAN A. TAYA[3], PANKAJ VARSHNEY[4]
[1]*Department of Electronics and Communication Engineering, Sri Krishna College of Engineering and Technology, Coimbatore, India*
[2]*Department of Electronics and Communication Engineering, Centre for IoT and AI (CITI), KPR Institute of Engineering and Technology, Coimbatore 641407, India*
[3]*Physics Department, Islamic University of Gaza, P.O. Box 108, Gaza, Palestine*
[4]*Department of Physics, SRM Institute of Science and Technology, Delhi-NCR Campus, Modinagar-201204, District-Ghaziabad, Uttar Pradesh, India*

In the present paper, we study one-dimensional superconductor photonic crystal composed of dielectric-superconductor multilayers. We use a well-known transfer matrix method approach to calculate transmission spectra. The optical allowed states between two photonic bandgap region is investigated as an optical multichannel filter application. We enhance our investigation to look at the impact of several factors, including thickness, angle of incidence and number of unit cells, on transmission spectra. The multichannel modes can be tuned with the geometrical parameters along with external parameter as the temperature.

(Received November 1, 2022; accepted April 7, 2023)

Keywords: Photonic crystal, Superconductor, Multichannel filter, Transfer matrix method

1. Introduction

Photonic crystals (PCs) are periodic structures of alternatively arranged dielectric materials, which give rise to photonic bandgaps (PBG)s [1,2]. PBG is originated due to periodic arrangement of dielectric or refractive index, similar to electronic bandgap in semiconductor. PCs are classified in three categories as one-dimensional (1D), two-dimensional (2D) and three-dimensional (3D) PC according to their periodicity [1,3,4]. 1D PC has periodic arrangement of dielectric along one direction only, while rest of two are homogeneous. Dielectric, semiconductor, metal, plasma, superconductor etc. are used and studied as material of 1D PC [5–14]. Due to the presence of PBG, the flow of photon can be controlled inside PC, which allows many potential applications as optical filter, switches, optical sensor, demultiplexer and so on [15–25].

Optical filter is one of the applications of PC, which can be studied be various researchers. As break in the regular periodic arrangement of dielectric causes a defect mode in PBG region [1,2,26]. Such defect mode has strong dependence on the parameter of defect layer, which can be used as optical filter application. The defect of large thickness gives number of defect modes, which can be studied as multichannel filters [27]. Kumar et al. reported TM mode filter application as multichannel at large angle [28]. Aly et al. investigated optical properties of meta-material and superconductor PBG with/without defect layer [29]. Aly et al. investigated optical spectra of 1D PC structure composed with superconducting material as defect layer sandwiched dielectric and semiconductor layers [30]. Aly et al. reported 1DPC as a semiconductor metamaterial in the near-infrared range, which is composed of Al-doped ZnO and ZnO [31].

In the present paper, we study a one-dimensional (1D) superconductor photonic crystal (SPC) consisting superconductor-dielectric multilayers. 1D SPC is studied as new approach as optical multichannel filter application using regular structure without defect layer and study the effect of various parameters on optical multichannel modes and externally tunable with temperature.

2. Theoretical model and method

Here, we consider a one-dimensional superconductor photonic crystal (1D SPC), which consist alternative dielectric and superconducting layers as shown in Fig. 1. The thickness of superconductor and dielectric layers are taken as d_A and d_B, respectively. The lattice constant or thickness of unit cell is defined as $a = d_A + d_B$.

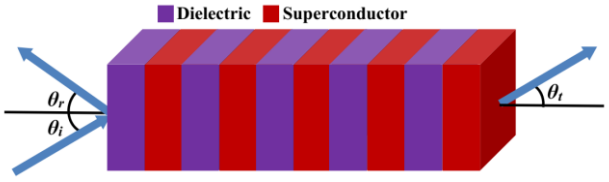

Fig. 1. Schematic Diagram of 1D SPC structure

The permittivity of superconductor depends on frequency of electromagnetic wave, which can be obtained using two fluid model at absolute zero temperature. The conductivity of superconductor is complex due to contribution of normal and superconducting electrons. The contribution of normal electron neglected in superconductor below critical temperature at zero magnetic field. Therefore, the conductivity of superconductor is given as [5,32,33].

$$\sigma(\omega) \approx -\frac{i}{\mu_0 \omega \lambda_L^2} \tag{1}$$

where λ_L is London-penetration depth, which is temperature dependent and given as [9,34]

$$\lambda_L(T) = \frac{\lambda_L(0)}{\left(1-\left(\frac{T}{T_c}\right)^4\right)^{1/2}} \tag{2}$$

where Tc is critical temperature and T is temperature on absolute scale. The temperature dependent refractive index of superconductor is obtained by

$$n_1 = \left[1 - \frac{c^2}{\omega^2 \left(\lambda_L(T)\right)^2}\right]^{\frac{1}{2}} \tag{3}$$

We use a well-known transfer matrix method (TMM) to calculate transmission, suitable for finite sized structure. The transfer matrix is obtained using boundary conditions of electric and magnetic fields in the form of a square matrix. The transfer matrix of j^{th} layer is given as [35,36]

$$M_j = \begin{bmatrix} \cos k_j d_j & \frac{i \sin k_j d_j}{p_j} \\ -i p_j \sin k_j d_j & \cos k_j d_j \end{bmatrix} \tag{4}$$

where $k_j = (2\pi/\lambda) n_j \cos\theta_j$ and $p_j = n_j \cos\theta_j$ for TE mode and $p_j = \cos\theta_j / n_j$ for TM mode. n_j is refractive index, d_j is thickness and θ_j is angle of propagation of j^{th} layer and λ is the wavelength. The characteristic transfer matrix of whole structure is achieved by simple multiplication of individual matrix of each layer, which is given as [35]

$$M = \prod_{j=1}^{N} M_j = \begin{bmatrix} M_{11} & M_{12} \\ M_{21} & M_{22} \end{bmatrix} \tag{5}$$

The transmission of 1D PC structure is given by

$$T = \left|\frac{p_i}{p_s}\right|^2 \left|\frac{2 p_i}{\left(M_{11} + p_s M_{12}\right) p_i + \left(M_{21} + p_s M_{22}\right)}\right|^2 \tag{6}$$

where $p_{i,s} = n_{i,s}\cos\theta_{i,s}$ for TE mode and $p_{i,s} = \cos\theta_{i,s}/n_{i,s}$ for TM mode.

3. Results and discussion

Here, we consider 1D SPC structure with periodic arrangement of Silicon as dielectric with refractive index 3.46 [37] and Tl-based high-temperature superconductor $Tl_2Ba_2Ca_2Cu_3O_{10}$ (Tl-2223) [38] layers alternatively as shown in Fig. 1. The geometrical parameters as thickness of superconductor layer (d_A) and thickness of silicon layer (d_B) are considered as 30 nm and 120 nm, respectively. The London-penetration (λ_L) at absolute zero temperature is taken as 163 nm and critical temperature (T_C) is taken as 121.5 K. The transmission spectra for 1D SPC is calculated using transfer matrix method using equation (6), which is as shown in Fig. 2. The transmission spectrum is plotted from visible to infrared (IR) region at low temperature as 70K.

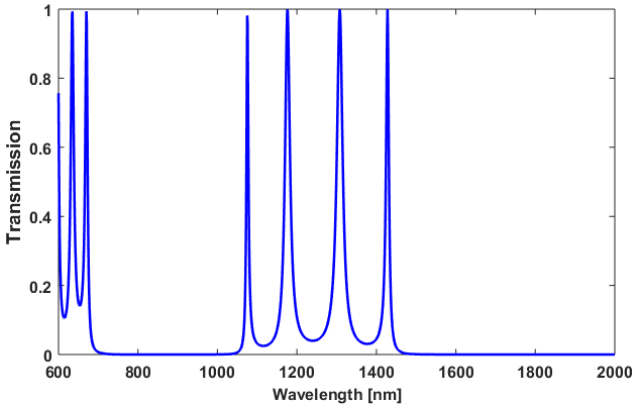

Fig. 2. The transmission spectrum for 1D SPC at temperature 70 K

From Fig. 2, it is clearly seen that one PBG obtained as 678-1078 nm and second higher photonic bandgap obtained from 1438 nm, which is cutoff wavelength. The cutoff wavelength is the highest wavelength after which propagation is not allowed through PC structure. There are some allowed wavelength modes are found between two photonic bandgap region. In the present study, we focus on such allowed wavelength modes between two PBGs, which can be used as an optical multichannel filter application. As the refractive index of materials (superconductor (Tl-2223) and silicon) varies with the temperature, which affects the multichannel modes with the temperature.

3.1. Effect of thickness

The thickness of multilayer structure can be used to tune the photonic bandgap region along with multichannel modes. In the present study, a bilayer structure is composed of superconductor and dielectric layers. Here, we study the effect of thicknesses (dielectric/

superconductor) on the optical transmission of multichannel modes. The study of thickness is divided in three part as follow

Variation in thickness of superconductor layer

In this case, we study the effect on the optical transmission of multichannel modes with the variation in thickness of superconductor layer (d_A), while the thickness of silicon layer (d_B) remains constant as d_B = 120 nm. The multichannel modes are calculated for different thicknesses of superconductor layer as d_A = 20 nm, 30 nm, 40 nm and 50 nm with the temperature as shown in Fig. 3.

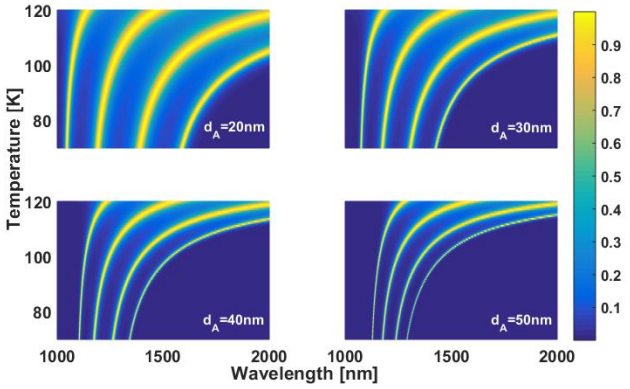

Fig. 3. Colormap transmission spectra of 1D SPC with wavelength and temperature for different thickness of superconductor layers d_A = 20 nm, 30 nm, 40 nm and 50 nm (color online)

From Fig. 3, it is clearly seen that the multichannel modes shift towards higher wavelength region and shows red shift with increase in temperature. As the thickness of superconductor (d_A) increases, the multichannel modes show shifting towards the higher wavelength region but the separation of multichannel reduces along with the width of individual modes.

Variation in thickness of dielectric layer

In this case, we study the effect on the optical transmission of multichannel modes with the variation in thickness of dielectric (silicon) layer (d_B), while the thickness of superconductor layer (d_A) remains constant as d_B = 30 nm. The optical multichannel modes are calculated for different thicknesses of silicon layer as d_B = 110 nm, 120 nm, 130 nm and 140 nm with the temperature as shown in Fig. 4. The optical multichannel modes show red shift with the temperature.

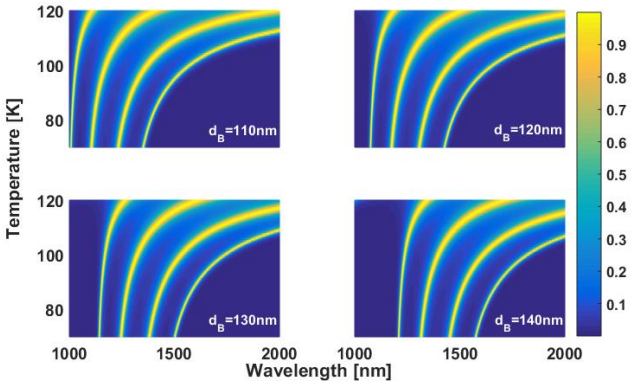

Fig. 4. Colormap transmission spectra of 1D SPC with wavelength and temperature for different thickness of silicon layer d_B = 110 nm, 120 nm, 130 nm and 140 nm (color online)

From Fig. 4, it is clearly seen that the optical multichannel modes show shifting towards higher wavelength region with an increase in the thickness of silicon layers. The separation between optical multichannel modes remains unchanged along with the width of individual channel with the variation in thickness of silicon layers. Therefore, the proper thickness of dielectric layers can be used to optical multichannel filter application of desired wavelength.

Variation in thicknesses of both superconductor and dielectric

In this case, we study the effect on the optical transmission multichannel modes with the variation in thickness of superconductor layer (d_A) and silicon layer (d_B), while the lattice constant remains unchanged as a = 150 nm. The optical multichannel modes are calculated for different thicknesses of superconductor layer as d_A = 20 nm, 30 nm, 40 nm and 50 nm with the temperature as shown in Fig. 5.

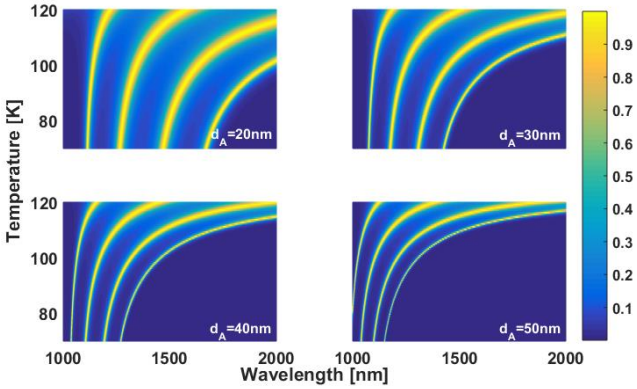

Fig. 5. Colormap transmission spectra of 1D SPC with wavelength and temperature for different thickness of superconductor layers d_A = 20 nm, 30 nm, 40 nm and 50 nm, while lattice constant a = 150 nm (color online)

Form Fig. 5, it is clearly seen that the optical multichannel modes show shifting towards lower wavelength region with an increase in the thickness of superconductor layer, while the thickness of silicon layer decrease for remain lattice constant unchanged as a = 150 nm. Here, the optical multichannel modes show blue shift while the separation between optical multichannel modes reduces with an increase in the thickness of superconductor layer with taking lattice constant unchanged. These results are completely different with previous two case of variation in the thickness of dielectric and superconductor layers. Therefore, the appropriate thicknesses of layers can be estimated using the present study to design an optical multichannel filter of desired wavelength and tune with externally with temperature.

3.2. Effect of angle of incidence

In this case, we study the effect of angle of incidence (θ) on the optical multichannel modes. As the angle of incidence become other than normal incident (0^o), the transverse electric (TE) and transverse magnetic (TM) mode get separate. For TE Mode, the transmission spectra at various angle of incidence are plotted as shown in Fig. 6 with temperature.

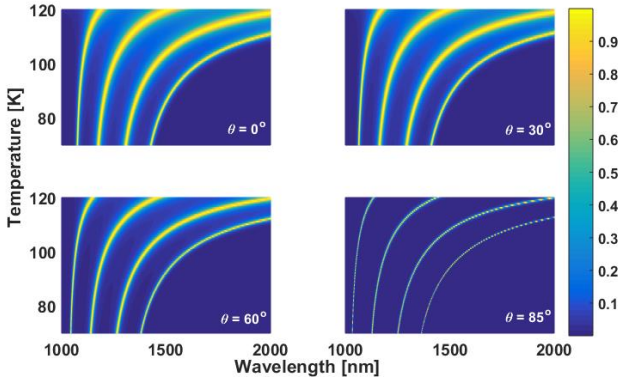

Fig. 6. Colormap transmission spectra of 1D SPC with wavelength and temperature for different angle of incidence $\theta = 0^o$, 30^o, 60^o and 85^o for TE mode (color online)

From Fig. 6, it is clearly seen that the separation between optical multichannel modes increases slightly with an increase in angle of incidence for TE mode. The width and the transmission peak of individual optical modes reduces with an increase in angle of incidence for TE mode. For the TM Mode, the optical transmission for multichannel modes are calculated and plotted at various angle of incidence with temperature as shown in Fig. 7.

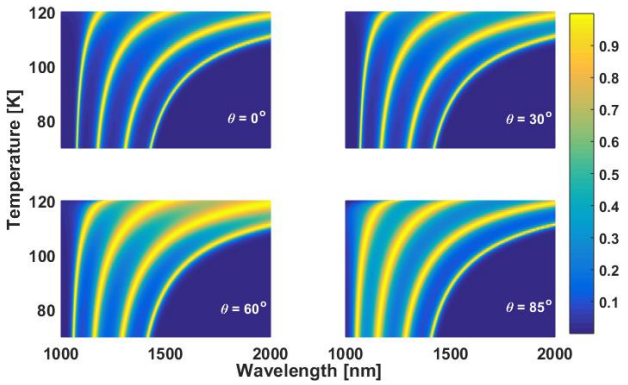

Fig. 7. Colormap transmission spectra of 1D SPC with wavelength and temperature for different angle of incidence $\theta = 0^o$, 30^o, 60^o and 85^o for TM mode (color online)

From Fig. 7, it is clearly seen that the separation between optical multichannel modes increases slightly, while the width and the optical transmission peak of an individual multichannel increases with an increase in angle of incidence upto 60^o and reduces for higher angle of incidence. As a result, TE mode is suitable for applications requiring narrow channel filters, but TM mode is suitable for those requiring optical multichannel filters with wide channels that are externally temperature-tunable.

3.3. Effect of Number of unit cells

In this case, we study the effect of number of unit cells (N) in 1D SPC. As, 1D SPC is composed of superconductor and dielectric layers as unit cell and repetition of unit cells construct whole structure. The number of unit cells uses to obtain the perfect photonic bandgap region with zero transmission. The optical transmission for different number of unit cells are plotted as shown in Fig. 8 with temperature.

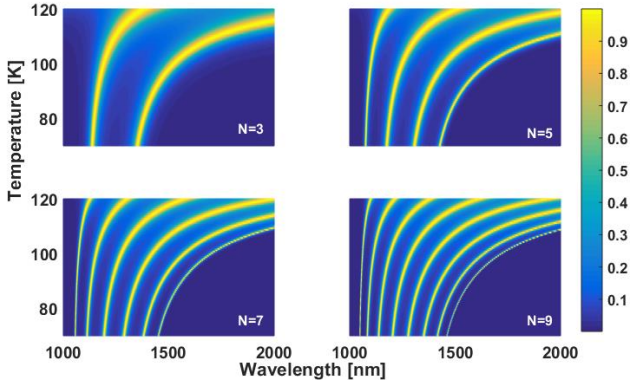

Fig. 8. Colormap transmission spectra of 1D SPC with wavelength and temperature for different number of unit cells as N = 3, 5, 7 and 9 (color online)

From Fig. 8, it is clearly seen that the number of optical multichannel increases with an increase in number of unit cell of 1D SPC structure. The number of multichannel modes are obtained as N-1 for 1D SPC structure. The separation between the optical multichannel modes reduces with the number of unit cells. It also observed that the optical channel near the cutoff wavelength (higher region) shows high tuning compared with the optical channel at higher wavelength edges. In this way, 1D SPC without any defect can be used as an optical tunable multichannel filter application with temperature. The desired optical multichannel filter modes can be achieved using appropriate parameters of structure.

4. Conclusion

In the present study, we investigated 1D SPC multilayered structure to obtain optical multichannel modes, which can be tuned externally with temperature. The optical multichannel modes shifted towards higher wavelength with an increase in the thickness of silicon layer, while became narrow with an increase in the thickness of superconductor layer. The optical multichannel modes shifted towards the lower wavelength with an increase in the thickness of superconductor layer while the lattice constant taken as unchanged. The optical transmission peak and width of the optical multichannel modes affected with the angle of incidence. The number of optical multichannel modes affected with the number of unit cells. In such way, 1D SPC without defect can be used for an optical tunable multichannel filter application.

References

[1] J. D. Joannopoulos, S. G. Johnson, J. N. Winn, R. D. Meade, Photonic Crystals: Molding the Flow of Light, Second (Princeton University Press, NJ, USA, 2011).

[2] N. Kumar, B. Suthar, Advances in Photonic Crystals and Devices, 1st Edition (CRC Press, Boca Raton, 2019).

[3] B. Suthar, A. K. Nagar, A. Bhargava, Chalcogenide Lett. **6**, 623 (2009).

[4] A. Bhargava, B. Suthar, Chalcogenide Lett. **6**, 529 (2009).

[5] G. Narayan Pandey, B. Suthar, Mater. Today Proc. (2021).

[6] A. Kumar, V. Kumar, B. Suthar, K. S. Singh, S. P. Ojha, Optik **125**, 393 (2014).

[7] A. H. Aly, H. A. Elsayed, Phys. Scr. **94**, 125501 (2019).

[8] B. Suthar, Optik **126**, 3429 (2015).

[9] G. N. Pandey, B. Suthar, N. Kumar, K. B. Thapa, J. Supercond. Nov. Magn. **34**, 2031 (2021).

[10] C. Nayak, A. Saha, A. Aghajamali, Indian J. Phys. **92**, 911 (2018).

[11] C. Nayak, C. H. Costa, K. V. P. Kumar, IEEE Trans. Plasma Sci. **48**, 2097 (2020).

[12] B. Suthar, A. Bhargava, Silicon **7**, 433 (2015).

[13] B. Suthar, G. N. Pandey, Macromol. Symp. **397**, 2000340 (2021).

[14] B. K. Paul, K. Ahmed, V. Dhasarathan, F. A. Al-Zahrani, M. N. Aktar, M. S. Uddin, A. H. Aly, Alexandria Eng. J. **59**, 5045 (2020).

[15] A. Aghajamali, C.-J. Wu, Appl. Opt. **55**, 2086 (2016).

[16] A. Kumar, V. Kumar, B. Suthar, M. Ojha, K. S. Singh, S. P. Ojha, IEEE Photonics Technol. Lett. **25**, 279 (2013).

[17] A. H. Aly, Z. A. Zaky, A. S. Shalaby, A. M. Ahmed, D. Vigneswaran, Phys. Scr. **95**, 035510 (2020).

[18] Z. Gharsallah, M. Najjar, B. Suthar, V. Janyani, Opt. Quantum Electron. **50**, 249 (2018).

[19] Ankita, B. Suthar, A. Bhargava, Plasmonics **16**, 59 (2021).

[20] B. Suthar, A. Bhargava, Silicon **13**, 1765 (2021).

[21] V. Kumar, B. Suthar, A. Kumar, K. S. Singh, A. Bhargava, Optik **124**, 2527 (2013).

[22] Ankita, S. Bissa, B. Suthar, C. Nayak, A. Bhargava, Results Opt. **9**, 100304 (2022).

[23] Ankita, S. Bissa, B. Suthar, A. Bhargava, J. Phys. Conf. Ser. (IOP Publishing) **2335**, 012006 (2022).

[24] B. Suthar, A. K. Nagar, A. Bhargava, J. Electron. Sci. Technol. **8**, 39 (2010).

[25] A. H. Aly, S. K. Awasthi, M. A. Mohaseb, Z. S. Matar, A. F. Amin, Cryst. **12**, 220 (2022).

[26] N. Kumar, K. B. Thapa, B. Suthar, editors, Photonic Crystals: Features and Applications (Nova Science Publishers, NY, USA, 2013).

[27] M. Solaimani, M. Ghalandari, A. Aghajamali, Optik **207**, 164476 (2020).

[28] V. Kumar, B. Suthar, A. Kumar, K. S. Singh, A. Bhargava, S. P. Ojha, Silicon **6**, 73 (2014).

[29] A. H. Aly, D. Mohamed, J. Supercond. Nov. Magn. **32**, 1897 (2019).

[30] A. H. Aly, S. E. S. A. Ghany, B. M. Kamal, D.Vigneswaran, Ceram. Int. **46**, 365 (2020).

[31] A. H. Aly, W. Sabra, J. Supercond. Nov. Magn. **29**, 1981 (2016).

[32] Z. A. Zaky, A. H. Aly, J. Supercond. Nov. Magn. **33**, 2983 (2020).

[33] F. Segovia-Chaves, H. Vinck-Posada, E. A. Gómez, Optik **209**, 164572 (2020).

[34] A. Aghajamali, Appl. Opt. **55**, 6336 (2016).

[35] P. Yeh, Optical Waves in Layered Media (John Wiley & Sons, NY, USA, 1988).

[36] B. Suthar, A. Bhargava, Opt. Commun. **285**, 1481 (2012).

[37] E. D. Palik, Handbook of Optical Constants of Solids (2012).

[38] C. K. Kim, A. Rakhimov, J. H. Yee, Phys. Rev. B - Condens. Matter Mater. Phys. **71**, 024518 (2005).

*Corresponding author: dhasa.viki@gmail.com